Journal of Nuclear Materials 390–391 (2009) 597–601

Contents lists available at ScienceDirect

Journal of Nuclear Materials

journal homepage: www.elsevier.com/locate/jnucmat

Experiments to measure hydrogen release from graphite walls during disruptions in DIII-D

E.M. Hollmann [a,*], N.A. Pablant [a], D.L. Rudakov [a], J.A. Boedo [a], N.H. Brooks [b], T.C. Jernigan [c], A.Yu. Pigarov [a]

[a] University of California, San Diego, La Jolla, CA 92093-0417, USA
[b] General Atomics, P.O. Box 85608, San Diego, CA 92186-5608, USA
[c] Oak Ridge National Laboratory, Oak Ridge, TN, USA

ARTICLE INFO

PACS:
52.55.Fa
52.40.Hf

ABSTRACT

Spectroscopy and wall tile bake-out measurements are performed in the DIII-D tokamak to estimate the amount of hydrogen stored in and released from the walls during disruptions. Both naturally occurring disruptions and disruptions induced by massive gas injection (MGI) are investigated. The measurements indicate that both types of disruptions cause a net release of order 10^{21} hydrogen (or deuterium) atoms from the graphite walls. This is comparable to the pre-disruptions plasma particle inventory, so the released hydrogen is important for accurate modeling of disruptions. However, the amount of hydrogen released is small compared to the total saturated wall inventory of order 10^{22}–10^{23}, so it appears that many disruptions are necessary to provide full pump-out of the vessel walls.

1. Introduction

Hydrogen and its isotopes are the primary working gases in tokamak experiments, so storage and release of hydrogen from the plasma-facing components (PFCs) has an important effect on tokamak fueling and density control [1]. In future tokamaks, understanding of hydrogen retention in PFCs will become even more crucial, due to the need to track tritium for fueling and safety considerations. Because of its excellent resistance to high heat fluxes, graphite is frequently used as a PFC, and its behavior in hydrogen has been studied extensively. In hydrogen discharges in tokamaks, graphite PFCs in high particle flux regions are found to saturate rapidly (within 10–100 ms) with hydrogen. The saturated layer typically has a deposition depth of order 50 nm and hydrogen content H/C $\approx$ 0.4/1, giving area densities of order 10^{21} H atoms/m^2 [2]. Over longer time periods (of order seconds), lower-flux regions also saturate with hydrogen. Also, co-deposition of sputtered C and H in cold PFC regions of net deposition can result in thick H layers, with co-deposited H/C layers of up to 1 mm in thickness being reported [3].

Very little is known about the release, migration, and re-deposition of PFC materials during fast transient events such as edge-localized modes (ELMs) and disruptions. During these events, plasma-wall fluxes can increase by many orders of magnitude over quiescent levels, possibly causing a significant change in erosion/deposition patterns. A large transient release of both carbon [4] and stored hydrogen [5] has been inferred indirectly on the DIII-D tokamak during disruptions, and the use of disruptions as a wall cleaning technique was attempted in TFTR [6]. Use of disruptions initiated by massive gas injection (MGI) as a method to remove tritium/carbon co-deposits in ITER has been suggested [7].

In the work presented here, measurements of hydrogen release from the walls of DIII-D during disruptions are presented. Two types of disruptions are studied: 'naturally' occurring disruptions which arise during normal operation due to hardware malfunctions or performance limits, and disruptions induced intentionally by MGI (massive gas injection of either hydrogen or neon). Overall, the measurements indicate a net release of order 10^{21} D or H particles during all types of disruptions; this is about the same size as the plasma particle inventory, but small compared with the total wall inventory ($\approx 10^{23}$ D or H particles).

2. Experiment hardware

A cross section view of DIII-D and schematics of some diagnostics used here is shown in Fig. 1. Most of the experiments discussed here used lower-single null H-mode discharges. All used D_2 as a fuel gas. A radially viewing CO_2 interferometer chord was used to measure plasma density during the disruptions. For the MGI-induced disruptions, a single fast valve was used to inject gas into the discharge. Either H_2 (about 1500 Torr-liter $\approx 5 \times 10^{22}$ H atoms in a 5 ms pulse) or Ne (about 1000 Torr-liter $\approx 3 \times 10^{22}$ Ne atoms in a 10 ms pulse) was used. To measure wall recycling of H and D, a slow (100 ms) high-resolution divertor spectrometer with six view chords across the lower divertor and two view chords

* Corresponding author.
E-mail address: ehollmann@ucsd.edu (E.M. Hollmann).

0022-3115/$ - see front matter © 2009 Published by Elsevier B.V.
doi:10.1016/j.jnucmat.2009.01.124

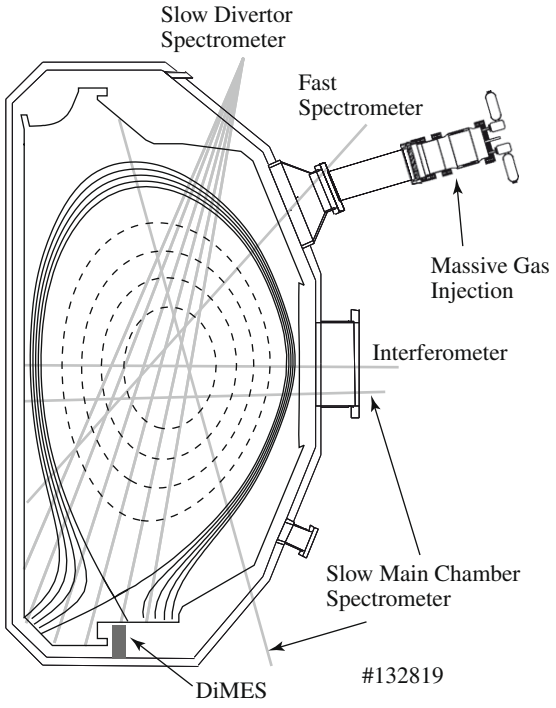

Fig. 1. DIII-D cross section showing main diagnostics used in this work.

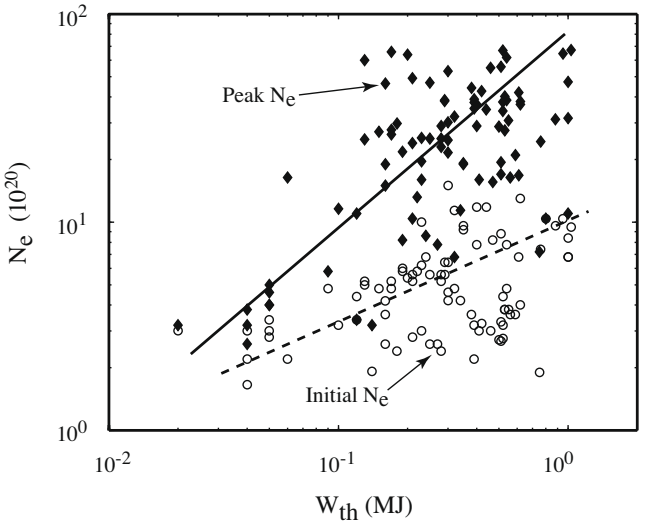

Fig. 2. Initial and peak plasma electron number during natural disruptions as a function of initial plasma thermal energy W_{th}.

across the main chamber was used, as was a fast (0.3 ms), single-chord spectrometer. Additionally, in one MGI experiment, the DiMES sample manipulator [8] was used to insert an $A = 18$ cm^2 graphite sample into the divertor floor.

3. Natural disruptions

Disruptions are characterized by a fast (~1 ms) thermal quench (TQ) phase where most of the plasma thermal energy is lost (often mostly to the divertor), followed by a slower (~5 ms) current quench (CQ) phase where the plasma magnetic energy is lost (often mostly to the main chamber). Electron density measurements taken during natural disruptions indicate that a significant transient release of particles into the plasma occurs during the disruptions. Fig. 2 shows the initial (pre-disruption) and peak (usually slightly after end of TQ) electron number measured with the interferometer. Disruptions which occurred during the operation period January–February of 2007 are shown. Although there is a significant scatter in the data, it can be seen that, on average, there is an increase of order 2–4 times in the plasma electron number (i.e. an increase of about 10^{21} electrons). An increasing trend with increasing plasma thermal energy is seen, i.e., higher energy plasmas tend to both store more electrons in the discharge and release more electrons from the wall when they disrupt.

0D modeling suggests that the observed increase in electron number comes dominantly from deuterium. During the TQ phase, the plasma is very anisotropic, with strong temperature and density gradients; however, in the CQ phase, the plasma is more well-mixed, and 0D modeling of the plasma current decay [9,10] is found to be reasonably successful at matching average plasma parameters. An example of this is shown in Fig. 3, where data and modeling of a natural disruption is shown. In the model, the plasma is initialized with the measured mean values of electron density n_e, electron temperature T_e, ion temperature T_i, and plasma current I_p. The measured initial carbon content of 2% is included; this is assumed to be entirely C^{6+}. The model unknowns are the rates of conducted heat loss to the walls, net rate of deuterium influx from the walls, and net rate of carbon influx from the walls; all these are assumed to be proportional to the plasma thermal energy W_{th}, with the three normalization constants varied as free parameters. The disruption simulation begins at time t_0. Charge-state resolved, non-equilibrium atomic physics (ionization, recombination, and radiation) including radiation trapping are included in the simulation [11]. The electron distribution is assumed to be Maxwellian, so runaway electron formation is neglected. Overall, it is found that matching the observed radiated power P_{rad} requires the addition of a small amount of sputtered carbon ($\approx 10^{20}$ C atoms). However, this added carbon does not cause sufficient n_e increase to match the data; for this, the addition of significant amounts of deuterium ($\approx 10^{21}$ D atoms) is required. This can be seen in Fig. 3(c), where the deuterium ion density n_D is seen to be more that 10 times larger than the carbon ion density n_C. Although recycling is ignored in the model (atoms added from the wall are assumed to remain in the plas-

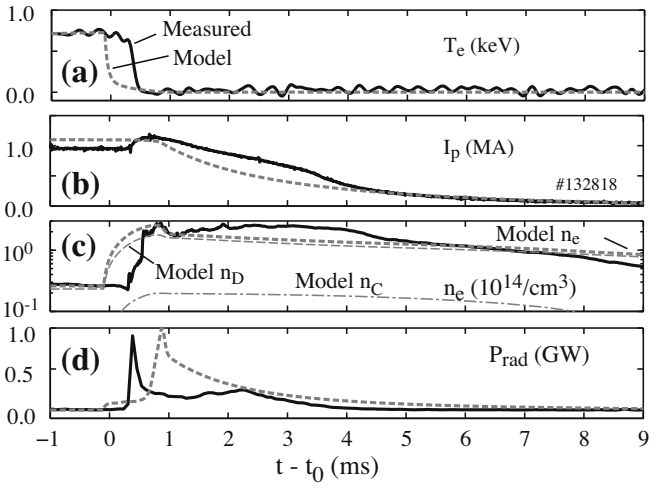

Fig. 3. Time traces of a natural disruption (solid lines) and 0D modeling (dashed lines) for (a) average electron temperature T_e, (b) plasma current I_p, (c) average electron density n_e (including modeled deuterium and carbon ion densities n_D and n_C), and (d) radiated power P_{rad}.

ma), it is expected that inclusion of recycling will not invalidate the need for a deuterium source term in the 0D modeling, since recycling produces no net increase in n_e. However, since recycling will allow each D to radiate multiple times (depending on how many times it is recycled during the disruption), it is expected that the amount of carbon influx needed to match P_{rad} in reality is less than predicted by the modeling. The small ~1 ms timing differences seen between modeling and experiment ([e.g. in T_e Fig. 3(a)] are thought to be due to 1D (radial transport) delays and do not significantly affect the conclusions drawn here.

Measurements of global particle inventory from vacuum chamber pumps also support that the observed increase in electron number comes dominantly from deuterium. Recycling ions (D^+) present in the disrupting plasma during the CQ phase are expected to mostly pump-out of the vacuum chamber as neutrals (D_2) rather than be embedded in the wall, since the plasma temperature is very low ($T_e \approx T_i \approx 5$ eV). Balancing the initial deuteron number in the plasma with the amount of gas pumped out of the vacuum chamber following a natural disruption typically indicates that of order 10^{21} extra deuterons are present from to wall release. Carbon, being non-recycling, would not be expected to be pumped out of the vacuum chamber following disruptions.

4. MGI-induced disruptions

To study wall release of hydrogen during MGI disruptions, a series of shots were shut down with MGI: two with H_2 MGI followed by four with Ne MGI. Initial (pre-disruption) wall conditions are not measured independently in these experiments; however, based on previous experience [5], we expect the walls to contain of order 10^{22}–10^{23} deuterons before the first MGI disruption. Wall release of H + D during the series shots is shown in Fig. 4(a). This is done using global particle balance (balancing sinks from pumps and plasma with sources from neutral beams and fueling lines) [5]. It can be seen that the walls tend to act as a sink (pumps) early in the shot (negative values) and sources later in the shot (positive values). This early wall pumping appears to be about 2 times larger following Ne MGI than following H_2 MGI, suggesting that Ne MGI is removing H and D from the walls more effectively. Wall release of H and D during the disruptions (not plotted) could not be calculated accurately using this technique since the vessel pressure and injected gas rate (from the MGI system) both become huge relative to the wall release (i.e. about 10^{23} atoms are injected with the MGI system and of order 10^{23} are seen to be pumped out of the chamber, so discerning the wall release of order 10^{21} from this data is very hard). The time axis shows cumulative shot time ignoring dead time between shots. Vertical gray lines show MGI shutdown times. Hydrogen recycling fluxes measured with the slow spectrometer are shown in Fig. 4(b)–(d). Total hydrogen fluxes shown in Fig. 4(b) and (c) are estimated from H_γ and D_γ brightness (at 434 nm) while total hydrogen fluxes from hydrocarbons shown in Fig. 4(d) are estimated from CH and CD brightness (with band heads around 431 nm). Rough conversions from measured brightness to hydrogen fluxes plotted in Fig. 4(b)–(d) are made using typical photon efficiency conversions or attached conditions ($S/XB \approx 1000$ for H_γ, D_γ [12], $(D/XB)^{CD_4\rightarrow CD} \approx 40$ for CD and $(D/XB)^{CH_4\rightarrow CH} \approx 30$ for CH [13]). Fluxes are integrated over the lower divertor area (≈6 m^2) to estimate divertor inflow or over the plasma surface area (≈20 m^2) to estimate main chamber inflow. It should also be noted that CH_4 production is a higher-order reaction than H_2 production, so direct comparison of H/D and CH/CD ratios is complicated and will not be attempted here. Despite the qualitative nature of the recycling measurements, several interesting trends can be seen in the data. Hydrogenic fluxes/recycling can be seen to be much (>10×) larger during H_2 MGI than Ne MGI. Following a single H_2 MGI disruption, a large H wall inventory is achieved, with comparable H vs. D fluxes in both divertor and main chamber seen during normal operation in the subsequent shot (before the disruption). Surprisingly, divertor hydrocarbon emission remains relatively small and unaffected both during and after the disruptions. For example, CH emission is much smaller than CD after the H_2 MGI, even though total H flux appears to be comparable. Although the H_2 MGI is clearly quite effective at embedding H_2 into the walls, neither Ne nor H_2 MGI appear to be especially effective at removing PFC hydrogen. In shots #132821 to #132824, a gradual decrease of divertor H emission (relative to D) during the shots can be seen; however, there is only one clear indication of stepwise decrease in the H/D ratio following Ne MGI: this is after shot #132823, where a significant (almost 2 times) drop in main chamber H fraction is observed.

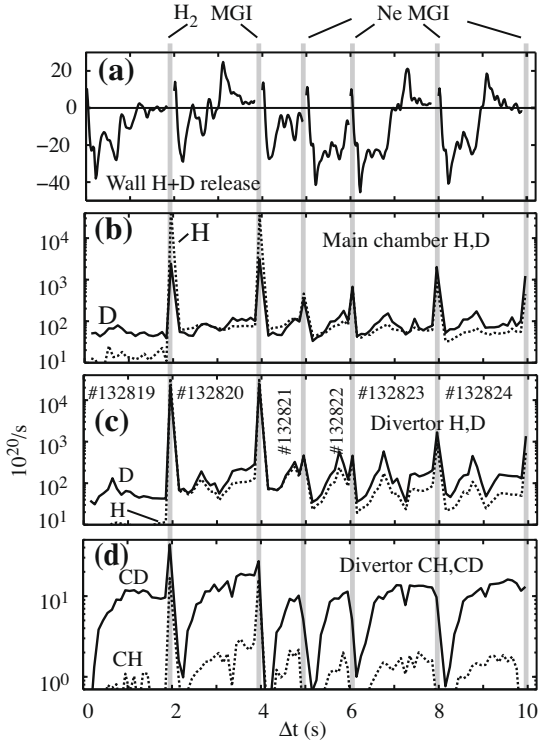

Fig. 4. (a) Wall release of hydrogen during shots estimated using global particle balance as well as hydrogen recycling inflow measured spectroscopically (b) in the main chamber by H_γ, D_γ brightness; (c) in the divertor by H_γ, D_γ; and (d) in the divertor by CH, CD. Six discharges are shown, each terminated with MGI. The time axis shows cumulative discharge time Δt .

In the data of Fig. 4(b)–(d), the spectrometer integration time was 100 ms and therefore integrates over both the TQ and CQ phases of the disruptions. This complicates interpretation of the data during the disruption since, for example, H_γ is expected to correspond dominantly to ionization radiation during the TQ and recombination radiation during the CQ. Separation of the TQ and CQ times was obtained with a single-chord fast spectrometer (dominantly viewing the main chamber). Fig. 5 shows (a) electron number N_e from the interferometer and (b) H_α and D_α emission measured with the fast spectrometer. In this shot #132819, the walls were initially loaded only with D, and the plasma contained about 5×10^{20} deuterium ions. At $t = 2000$ ms the shot was shut down with H_2 MGI. In the middle of the CQ phase ($t \approx 2006$–2010 ms), where the plasma is expected to be reasonably well-mixed, the deuteron number in the plasma N_D can be estimated from the measured D_α fraction: $N_D \approx N_e(D_\alpha/D_\alpha + H_\alpha)$. This is shown with the gray curve in Fig. 5(a). Overall, the data suggest $N_D \approx 10^{21}$ during the CQ, consistent with a net release of about

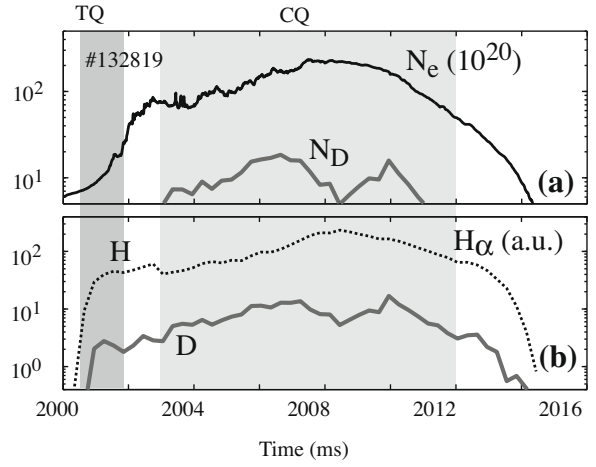

Fig. 5. (a) Measured electron number N_e (black curve) and deuterium ion number estimated from (b) measured H_α and D_α brightness. Shaded regions mark thermal quench (TQ) and current quench (CQ).

5×10^{20} deuterons from the wall, probably mostly during the TQ, where the largest rise in N_e is seen.

To measure the amount of deuterium stored in the graphite wall directly, a graphite sample was inserted using the DiMES sample manipulator. Two separate exposures were performed: in the first, the sample was exposed to three normal D_2 discharges, transferred under argon to a bake-out chamber and baked out at 1000 °C for 1.5 h to measure the deuterium content (seen as HD and D_2 in an RGA). In the second exposure, the sample was again exposed to three D_2 discharges, the last of which was terminated with H_2 MGI. The bake-out pressure traces of the two samples, shown in Fig. 6, are seen to be roughly similar. A calibrated D_2 leak was used to calibrate the pressure traces, giving about 3.7×10^{18} D atoms in the MGI case and 2.0×10^{18} D atoms in the non-MGI case; from the sample area of 18 cm^2, this gives area densities of 2.0×10^{21} and 1.1×10^{21} atoms/m^2, consistent with expected saturation densities of order 10^{21} atoms/m^2. Although statistics could not be gathered here, this factor of two variation is probably within the shot-shot variation (based on experience in PISCES with bake-out of samples exposed to steady D_2 plasmas), so we conclude that the net D release from H_2 MGI is relatively small. Hydrogen background levels in the bake-out chamber were too large to accurately measure H_2 stored in the samples.

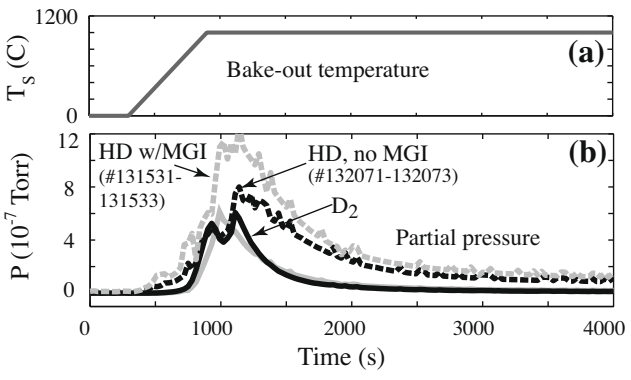

Fig. 6. Bake-out traces of graphite DiMES samples exposed to D_2 discharges with (gray) and without (black) H_2 MGI, showing partial pressure of HD (dashed curves) and D_2 (solid curves).

5. Discussion

The area density of D measured with the DiMES bake-out after only three shots exposure ($\approx 1-2 \times 10^{21}$ D/m^2) is consistent with expected saturation densities ($\approx 10^{21}$ D/m^2) and, multiplied by the wall area of 70 m^2, gives a wall inventory $\approx 10^{23}$ consistent with pumping measurements in DIII-D [5]. Assuming only the divertor wall region is saturated with D, the wall inventory is still quite large, $\approx 10^{22}$. During disruptions, very large recycling fluxes are observed, but a surprisingly small fraction ($\sim$1%) of the wall inventory appears to be ultimately lost and pumped away. For example, in H_2 MGI disruptions, of order 10^{23} hydrogen atoms are injected into the vacuum chamber and recycling inflows of order 10^{23} are observed in both main chamber and divertor (as seen in Fig. 4(b)–(c) taking 10^{24}/s times 0.1 s integration time). These large hydrogen fluxes do not appear to result in a large net loss of D from the wall, with a net $\approx 10^{21}$ deuterons lost from the wall suggested in Fig. 5(a) (consistent with Fig. 2) and no net loss of D seen in Fig. 6. The large D spikes seen during H_2 MGI shots in Fig. 4(a) and (b) when compared with Ne MGI shots seem to indicate the more efficient removal of wall-stored D due to H_2 MGI; however, this seems to be contradicted by the greater wall pumping seen following Ne MGI vs. H_2 MGI, seen in Fig. 4(a). Hydrogen implantation appears to be easier than hydrogen removal, as after a single H_2 MGI shot, the PFC H/D $\sim$ 1, with the ratio still being H/D $\sim$ 1/2 after several shots terminated with Ne MGI disruptions, Fig. 4(c). There is some evidence for net removal of D from the main chamber following Ne MGI. Whether this removal is due to particle fluxes or due to wall heating cannot be determined from this data. Also, the present data cannot rule out the possibility that some fraction of the decreasing trend in H recycling seen in Fig. 4(b) and (c) is actually due to H being covered by carbon co-deposits rather than a net removal of H from the vessel walls. Chemical erosion as measured by CD band emission (which is thought to arise dominantly as a result of CD_4 release from the wall) does not appear to be significantly affected by MGI disruptions, nor does it appear to account for the measured release of hydrogen during the disruptions.

6. Conclusion

In conclusion, these measurements indicate that PFC release of hydrogen is important for accurate modeling of disruptions in tokamaks with graphite walls, with of order the initial plasma particle inventory ($\approx 10^{21}$ H or D particles) released from the wall by each disruption. However, this is small compared with the total wall inventory ($\approx 10^{23}$ H or D particles), so disruptions (natural or MGI-induced) do not appear to be extremely efficient at cleaning existing hydrogen out of PFCs; although they may serve as a useful complement to other wall cleaning techniques. This situation may change in future large tokamaks like ITER, however, where wall area will be $\approx 10\times$ larger than DIII-D but stored thermal energy will be $\approx$400 times larger, while disruption TQ time scales are expected to be only somewhat (perhaps $\approx$ 2 times) slower. Wall heating during disruptions is thus expected to be much larger, presumably resulting in greater thermal desorption of H from the wall. Better diagnosed disruptions experiments and modeling (including different wall materials such as Be and W) will be necessary to predict the level of H release from the walls of these larger tokamaks during disruptions.

Acknowledgements

This work supported by the US Department of Energy under DE-FC02-04ER54698, DE-FG02-07ER54917 and DE-AC05-00OR22725.

Assistance of Drs M. Baldwin, J. Hanna, G. Temmerman, and K. Umstader in using the PISCES lab TDS system is acknowledged.

References

[1] J. Winter, Plasma Phys. Contr. Fus. 36 (1994) B263.
[2] G. Federici, C.H. Skinner, J.N. Brooks, et al., Nucl. Fus. 41 (2001) 1968.
[3] M. Mayer, V. Phillips, P. Wienhold, et al., J. Nucl. Mater. 290 (2001) 381.
[4] E.M. Hollmann, D.S. Gray, D.G. Whyte, et al., Phys. Plasma 10 (2003) 2863.
[5] R. Maingi, G.L. Jackson, M.R. Wade, et al., Nucl. Fus. 36 (1996) 245.
[6] H.F. Dylla et al., J. Nucl. Mater. 145 (1987) 48.
[7] D.G. Whyte, J.W. Davis, J. Nucl. Mater. 337 (2005) 560.
[8] C.P.C. Wong, D.L. Rudakov, J.P. Allain, et al., J. Nucl. Mater. 363 (2007) 276.
[9] D.G. Whyte, T.C. Jernigan, D.A. Humphreys, et al., J. Nucl. Mater. 313 (2003) 1239.
[10] E.M. Hollmann, P.B. Parks, H.A. Scott, Contr. Plasma Phys. 48 (2008) 260.
[11] E.M. Hollmann, T.C. Jernigan, P.B. Parks, et al., Nucl. Fus. 48 (2008) 11507.
[12] R.K. Janev, D. Reiter, U. Samm, Collision Processes in Low-temperature Hydrogen Plasmas, Jul-4105, Forzchungszentrum Juelich, 2003.
[13] S. Brezinsek, A. Pospieszczk, D. Borodin, et al., J. Nucl. Mater. 363 (2007) 1119.